Polymer 50 (2009) 491–498

Contents lists available at ScienceDirect

Polymer

journal homepage: www.elsevier.com/locate/polymer

Synthesis of azopolymers with controlled structure and photoinduced birefringence in their LB films

Felippe J. Pavinatto*, Juliana Y. Barletta, Rafaela C. Sanfelice, Marcos R. Cardoso, Débora T. Balogh, Cleber R. Mendonça, Osvaldo N. Oliveira, Jr.

Universidade de São Paulo, Instituto de Física de São Carlos, Av. Trabalhador São Carlense 400, CP 369, 13566-590 São Carlos, São Paulo, Brazil

ARTICLE INFO

Article history:
Received 17 September 2008
Received in revised form
14 November 2008
Accepted 17 November 2008
Available online 30 November 2008

Keywords:
ATRP
Block-copolymers
Optical birefringence

ABSTRACT

The molecular architecture of azopolymers may be controlled via chemical synthesis and with selection of a suitable film-forming method, which is important for improving their properties for practical uses. Here we address the main challenge of combining the photoinduced birefringence features of azopolymers with the higher thermal and mechanical stabilities of poly(methyl methacrylate) (PMMA) using Atom Transfer Radical Polymerization (ATRP) to synthesize diblock- and triblock-copolymers of an azomonomer and the monomer methyl methacrylate. Langmuir–Blodgett (LB) films made with the copolymers mixed with cadmium stearate displayed essentially the same optically induced birefringence characteristics, in terms of maximum and residual birefringence and time for writing, as the mixed LB films with the homopolymer poly[4-(*N*-ethyl-*N*-(2-methacryloxyethyl))amino-2′-chloro-4′-nitro-azobenzene] (HPDR13), also synthesized via ATRP. In fact, the controlled architecture of HPDR13 chains led to Langmuir films that could be more closely packed and reach higher collapse pressures than the corresponding films obtained with HPDR13-conv synthesized via conventional radicalar polymerization. This allowed LB films to be fabricated from neat HPDR13, which was not possible with HPDR13-conv. The enhanced organization in the LB films produced with controlled azopolymer chains, however, led to a smaller free volume available for isomerization of the azochromophores, thus yielding a lower photoinduced birefringence than in the HPDR13-conv films. The combination of ATRP synthesis and LB technology is then promising to obtain optical storage in films with improved thermal and mechanical processabilities, though a further degree of control must be sought to exploit film organization while maintaining the necessary free volume in the films.

1. Introduction

Azopolymers have been widely studied in recent years because of their interesting properties that arise from the photoinduced isomerization of the azo N═N group, which allows for a variety of applications, including optical storage and surface relief gratings (SRGs) [1]. The principal feature in thin films of azopolymers is the photoalignment induced by polarized light with sequential azo *trans–cis–trans* isomerization cycles, leading to optical anisotropy (birefringence) and mass transport. The efficiency and stability of the photoisomerization depend on polymer properties such as the azogroup mobility [2], the chemical composition of the azo moiety [3], free volume around the azogroup [4] and film thickness [5]. Furthermore, two of the most important factors, which were explored in the present work, are the film architecture and the controlled polymer microstructure, represented by the relative position of the chromophores in the chain, low polydispersity and chain linearity.

A useful polymer microstructure is that of block-copolymers (BCs), with which specific properties of different polymers can be combined in a single compound. Although BCs have been exploited in several areas [6], only a few studies had been reported on azobenzene containing block-copolymers (AzoBCs) until few years ago, being practically restricted to grafted di- or triblock-copolymers [7,8]. With the advent of controlled radical polymerizations such as Atom Transfer Radical Polymerization (ATRP), AzoBCs now receive more attention since a wider range of monomers can be polymerized [9]. Indeed, amphiphilic AzoBCs synthesized with ATRP have been exploited in photoactive vesicles and micelles [10–14], while liquid-crystalline (LC) homopolymers and AzoBCs are used as photoresponsive thermoplastic elastomers [15,16]. Systematic studies on self-assembled nanostructures from azo-containing BCs are especially attractive, given the considerable interest generated by phase segregation in this class of materials [17–21], which can be allied to photoalignment effects [7,22–25]. The confinement by phase segregation has been found to alter the mesogenic properties

* Corresponding author. Tel./fax: +55 16 3373 9825.
E-mail address: pavinatto@ifsc.usp.br (F.J. Pavinatto).

0032-3861/$ – see front matter © 2008 Elsevier Ltd. All rights reserved.
doi:10.1016/j.polymer.2008.11.043

and reduce or even suppress thermochromism on LC azopolymers [26,27]. Also suggested were constraints imposed by phase segregation on the photoalignment of the azo-units, resulting in low birefringence levels.

There have also been attempts to photoalign azochromophores in block-copolymers. For instance, Forcén et al. reported the synthesis of diblock-copolymers of PMMA with a methacrylic azomonomer containing a mesogenic cyano-azobenzene [28,29], yielding less absorptive azopolymers for the fabrication of uniform holographic gratings. Spin-coated, phase-segregated films of copolymers with 7 and 20% of azomonomers in the chain were produced, and stable photoinduced birefringence and holographic gratings were obtained only with the block-copolymer having the highest content of azomonomer. Most of the important features of the holographic gratings, e.g. maximum birefringence and effectiveness of recording, were better than for random copolymers.

To our knowledge there has been no report on the effects from the controlled microstructure, inherent in block-copolymers, and film architecture on the optically induced birefringence. In this paper we report on the synthesis via ATRP of a homopolymer containing the pseudo-stilbene azochromophore Disperse Red 13, and of diblock- and triblock-copolymers of the azomonomer with methyl methacrylate (MMA). The control over the molecular structure of the macromolecules and film architecture was exploited in producing Langmuir–Blodgett (LB) films, whose optically induced birefringence was investigated. Non-LC azopolymer and non-phase-segregated films were applied to evaluate only structural and microstructural effects. LB films from the homopolymer and block-copolymers were used, with results for a conventionally synthesized homopolymer being employed for comparison. It will be shown that pure and easy-to-form LB films were built from poly[4-(*N*-ethyl-*N*-(2-methacryloxyethyl))amino-2′-chloro-4′-nitroazobenzene] (HPDR13) synthesized via ATRP, and that the induced birefringence features from homopolymers can be preserved in the LB films of block-copolymers.

2. Experimental section

2.1. Materials and characterizations

All chemicals were purchased from Aldrich or Merck. Methyl methacrylate (MMA) and tetrahydrofuran (THF) were previously distilled. The azomonomer [4-(*N*-ethyl-*N*-(2-methacryloxyethyl))amino-2′-chloro-4′-nitroazobenzene] (DR13MA) was synthesized by esterification reaction of the azodye Disperse Red 13 (DR13) with methacryloyl chloride, following procedures from the literature [30]. Copper(I)chloride (CuCl) was purified by washing with glacial acetic acid, followed by absolute ethanol and ethyl ether. Ethyl-2-bromobutyrate (EBB), dimethyl-2,6-dibromoheptanedioate (DBI) and 1,1,4,7,10,10-hexamethyltriethylenetetramine (HMTETA) were used as-received. The FTIR spectra of the polymers were recorded on a Thermo Nicolet-Nexus 470 equipment in the transmission mode. The measurements were made on films cast from chloroform solutions onto NaCl windows. ^{1}H NMR spectra were recorded on a Bruker 200 MHz spectrometer in $CDCl_3$ solutions. Molecular weights and polydispersity indexes were measured by size exclusion chromatography (SEC) using an Agilent 1100 system with PL-Gel mixed-B and mixed-C columns, THF as eluent (1.0 mL/min at 35 °C), refractive index detector and polystyrene standards. Differential scanning calorimetry (DSC) measurements to determine the glass transition temperature, T_g, of the samples were conducted in a temperature range from 25 to 250 °C, with a heating rate of 10 °C/min, in a TA Instruments DSC2910 equipment. Relaxation temperatures were taken from the second scanning, with the first run used to release induced stress from the materials.

2.2. ATRP synthesis

The homopolymerization of DR13MA was performed as follows: to a 10 mL glass ampoule, 26.0 mg of CuCl (2.63×10^{-4} mol), 66 μL (2.43×10^{-4} mol) of HMTETA and 2.0 mL of THF were added and the ampoule was evacuated, purged with nitrogen and stirred to form the catalytic complex (noticed by the color of the solution that turned light green). Then, 404.0 mg of DR13MA monomer (9.66×10^{-4} mol) and 18 μL of the initiator EBB (1.22×10^{-4} mol) were added, with additional 3.0 mL of solvent. Three freeze–pump–thaw cycles were performed to remove residual oxygen and the ampoule was sealed under vacuum. The reaction was allowed to stand at 65 °C for 24 h in an oven. After cooling, the ampoule contents were diluted with THF and passed through a basic alumina column to remove the catalyst. The filtrate was concentrated and the polymer was precipitated into a large excess of *n*-hexane. ^{1}H NMR assignments for the homopolymer were: 0.90 ppm (2H, backbone CH_2), 1.25 ppm (3H, CH$_2$–CH_3), 1.85 ppm (3H, α-CH_3), 3.46 ppm (2H, N–CH_2–CH$_3$), 3.64 ppm (2H, N–CH_2–CH$_2$–O), 4.08 ppm (2H, O–CH_2), 6.74 ppm (2H, $H_{2,6}$), 7.64 ppm (1H, $H_{6'}$), 7.84 ppm (2H, $H_{3,5}$), 8.05 ppm (1H, $H_{5'}$) e 8.32 ppm (1H, $H_{3'}$).

To produce diblock- and triblock-copolymers, ATRP of DR13MA was initiated with previously produced monofunctional (PMMA–Cl) and difunctional (Cl–PMMA–Cl) macroinitiators, respectively, samples BL-A and BL-B in Table 1. Other reactants and reaction conditions were the same as for the homopolymerization. The amounts of CuCl and HMTETA were adjusted to obtain a macroinitiator:CuCl:HMTETA feed molar ratio of 1:1:1, and 5 mL of THF was used as solvent. The diblock-copolymer PMMA-*b*-DR13 and triblock-copolymer DR13–PMMA–DR13 were purified, similarly to the homopolymer, through repeated solution–precipitation cycles in THF and *n*-hexane. All syntheses were carried out in duplicates and showed to be reproducible. The diblock-copolymer is referred to as DBL and the triblock-copolymer TBL.

As shown in the table, the polydispersity for HPDR13 (1.65) is not as low as in some polymers synthesized via ATRP. We did try to optimize the synthesis of the homo- and block-copolymers. However, such attempts failed, probably owing to complexation of the azo-unit with the ATRP copper catalyst.

2.3. Langmuir–Blodgett (LB) experiments

Langmuir and Langmuir–Blodgett (LB) experiments were carried out on a KSV 5000 trough housed in a class 10,000 clean room. Ultrapure water supplied by a Milli-RO coupled to a Milli-Q purification system (Millipore, resistivity 18.2 MΩ-cm, pH 6.0) was used as subphase. The spreading solutions were prepared from HPLC grade chloroform with a typical concentration of 0.2–1.0 mg/mL. The subphase temperature was 22.0 °C (room temperature) and Langmuir films were compressed at a barrier speed of 20 mm/min in all measurements. Surface pressure *versus* area (π–A) isotherms were monitored by an electronic balance, using

Table 1
Homopolymerization of DR13MA and block-copolymerization with MMA by ATRP.

Sample[a]	Initiator (mol)	$[DR13MA]_0/[I]_0$[b]	M_n[c] (g/mol)	M_w/M_n[c]	Azo %[d]
HPDR13	EBB (1.22×10^{-4})	7.88	4000	1.65	100.0
BL-A	EBB (6.80×10^{-4})	–	20,200	1.11	–
BL-B	DBI (1.15×10^{-4})	–	19,700	1.40	–
DBL	BL-A (3.05×10^{-5})	7.87	24,790	1.21	6.5
TBL	BL-B (5.07×10^{-6})	28.20	24,900	1.22	12.0

[a] HPDR13 – homopolymer; BL-A – monofunctional macroinitiator PMMA–Cl; BL-B – difunctional macroinitiator Cl–PMMA–Cl; DBL – diblock-copolymer PMMA-*b*-DR13; TBL – triblock-copolymer DR13-*b*-PMMA-*b*-DR13.
[b] Feed molar ratio of DR13MA, $[DR13MA]_0$ and Initiator, $[I]_0$.
[c] Determined by SEC on the basis of polystyrene standards.
[d] Azo percentage in weight, estimated by UV–vis spectroscopy.

a Wilhelmy plate made of filter paper. The mean molecular area values were calculated based on the molecular weight of the polymer repeating unit. For the diblock- and triblock-copolymers, the mean molecular areas were calculated using an average molecular weight obtained from the composition ratio of the block-copolymer, which was determined with UV–vis spectroscopy. Langmuir–Blodgett (LB) films were deposited onto BK7 hydrophilic glass slides at a dipping speed of 1 mm/min. For the deposition of mixed LB films cadmium chloride (4×10^{-4} M) and sodium bicarbonate (5×10^{-5} M – to keep the pH at 6.0) were dissolved in the aqueous subphase, and stearic acid was added to the chloroform solution at the ratio of 1:1 in weight. The film thickness was determined by profilometry using a Talystep equipment from Taylor-Hobson.

2.4. Optical measurements

The experimental setup for the photoinduced birefringence experiments is described in Ref. [31], and only a few details will be given here. Optical birefringence was induced in the sample by a continuous-wave, linearly polarized Ar^+ laser operating at 514 nm (writing beam). To probe the birefringence during the writing laser exposure, we measured the transmission of a low power, linearly polarized laser (reading beam) through the sample, which is placed between two crossed polarizers. The wavelength of the reading beam is chosen in the non-absorptive region of the azochromophores; in general a He–Ne laser operating at 632.8 nm is used. The polarization angle of the writing beam is set at 45° with respect to the polarization of the reading beam.

The optically induced birefringence, Δn, can be calculated from the reading beam transmission, T, using

$$\Delta n = \lambda/\pi d \sin^{-1}\sqrt{T}$$

where λ is the wavelength of the incident radiation, and d is the film thickness.

3. Results and discussion

3.1. Synthesis and characterization

3.1.1. Homopolymer HPDR13

ATRP was used to synthesize an azo homopolymer (HPDR13) and diblock- and triblock-copolymers of DR13MA and MMA, with the main aim of obtaining polymers with controlled structures and microstructures. Kinetics studies were not performed to optimize the synthesis conditions or to confirm its livingness. For the homopolymer, the halide exchange between the initiator (bromated) and the catalyst (chlorinated) was used to obtain better control over the ATRP equilibrium [32]. The monomer:initiator molar ratio was arbitrarily chosen as 7.8:1 for the homopolymer and diblock-copolymer synthesis. A high monomer-to-initiator ratio was chosen for the triblock-copolymer synthesis (28.2:1, Table 1) because each macroinitiator chain has two sites for polymer growth. In addition, the increase of four times in the quantity of monomer was motivated by the low efficiency of azomonomer incorporation observed in the diblock-copolymer synthesis (discussed below). The chemical structures proposed for the materials are shown in Fig. 1.

HPDR13 has already been synthesized by conventional radical polymerization in our group [30]; this material is hereafter referred to as HPDR13-conv. Results from chemical characterizations of HPDR13 are essentially identical to that from HPDR13-conv, which confirms that the same chemical structure was produced with ATRP. The UV–vis absorption band for the polymer, related to the azobenzene π–π^* transition, is centered at 475 nm. The FTIR

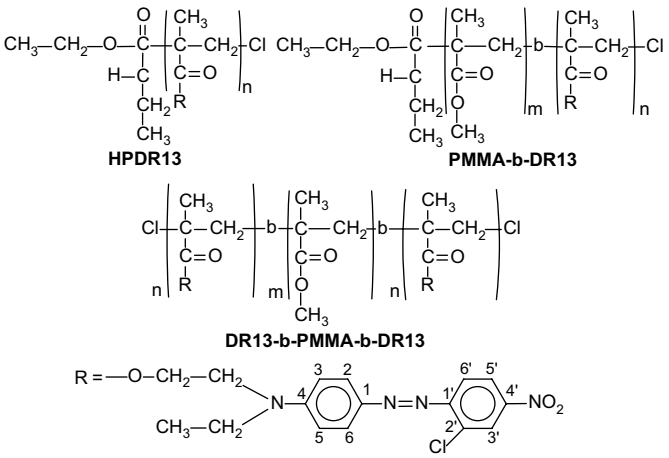

Fig. 1. Repeat units of HPDR13 homopolymer, PMMA-*b*-DR13 diblock-copolymer and DR13-*b*-PMMA-*b*-DR13 triblock-copolymer. Cl is the chlorinated active chain end. In the case of the triblock-copolymer, the initiator (DBI) fragment, located around the center of the PMMA block, is omitted.

spectrum (not shown) contains as major bands those from aromatic stretching at 1598 cm^{-1}, ester C–C–O symmetric stretching at 1138 cm^{-1} and NO_2 stretching at 1336 cm^{-1}, which confirms the integrity of DR13 moiety after polymerization. ^1H NMR peak assignments, given in Section 2, are the same as those from HPDR13-conv described in Ref. [30].

The SEC curve for HPDR13 shows that the homopolymerization has occurred in a poorly controlled fashion, with the polydispersity, 1.65, being larger than that usually observed for ATRP polymers. This uncontrolled characteristic can be attributed to some possible coupling between the tertiary amine of DR13 and the catalytic metal center, which is known to occur for nitrogen-containing monomers [33,34]. The M_n obtained for the polymer was ca. 4000 g/mol, which is much higher than the theoretical M_n calculated for the $[DR13MA]_0/[I]_0$ ratio used (1546 g/mol) [15]. Although the result for the ATRP synthesis was not ideal, for the purpose of our work, i.e. to produce controlled structures, it is satisfactory. The SEC curve shows no bimodality and the PDI index is about half the value for HPDR13-conv (PDI ca. 2.9). Moreover, the yield of pure polymer in ATRP (41% in weight) is twice that of usually obtained in the conventional radical synthesis. The good reproducibility of the ATRP synthesis was confirmed in a replica of the synthesis, as mentioned before. Therefore, ATRP is advantageous for synthesizing HPDR13, even with non-optimized conditions.

3.1.2. Block-copolymers *PMMA*-b-*DR13* and *DR13*-b-*PMMA*-b-*DR13*

Diblock- and triblock-copolymers with HPDR13 as a photoactive segment and poly(methyl methacrylate) (PMMA) as an optically inert segment were synthesized for the first time in this work. The procedures for synthesizing PMMA-*b*-DR13 and DR13-*b*-PMMA-*b*-DR13 were reproducible. The yield for DBL was ca. 60%, as determined from the mass retrieved from the synthesis, while for TBL the yield was approximately 15%. The main characteristics of the block-copolymers are summarized in Table 1. The SEC curves for DBL and TBL are shown respectively in Fig. 2A and B together with the traces of the macroinitiators used in the synthesis, BL-A (PMMA–Cl) for DBL and BL-B (Cl–PMMA–Cl) for TBL.

The SEC traces for block-copolymers are shifted to higher molecular weights compared to those of the macroinitiators. For DBL a shoulder centered at a molecular weight twice that of the main peak appeared, pointing to some coupling termination reactions. The polydispersity of the resulting diblock-copolymer increased only slightly in comparison with the macroinitiator. For

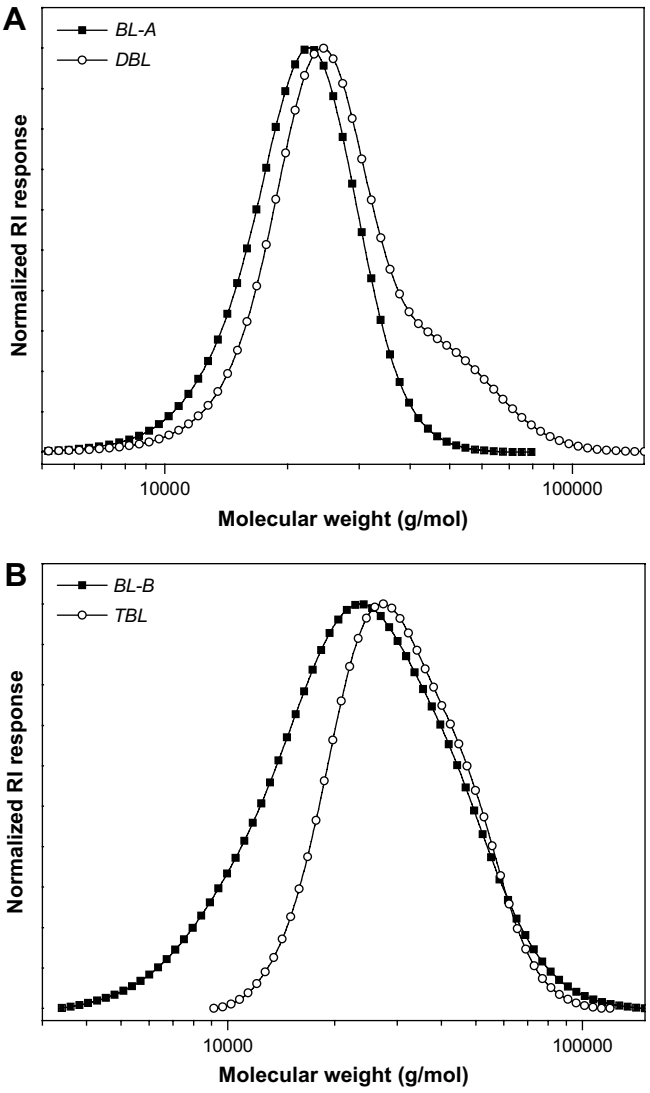

Fig. 2. SEC traces: [A] for the diblock-copolymer PMMA-*b*-DR13 (DBL) and its macroinitiator PMMA–Cl (BL-A); and [B] for the triblock-copolymer DR13-*b*-PMMA-*b*-DR13 (TBL) and the corresponding macroinitiator Cl–PMMA–Cl (BL-B).

the triblock-copolymer TBL a slight overlap occurs with the trace of the macroinitiator BL-B. However, the molecular weight distribution is narrower with PDI decreasing from 1.40 to 1.22. Interestingly, when using PMMA as macroinitiator in the ATRP of the DR13 azomonomer, the reaction seems to succeed in a more controlled fashion, with PDI indexes consistent with those from controlled radical polymerizations. We can speculate that the increased viscosity of the medium may hinder the complexation between azomonomer and catalyst, which we suppose to occur in the homopolymerization. Indeed, specifically in the case of TBL, some loss of macroinitiator during purification may have contributed to narrowing the size distribution.

DBL and TBL were also characterized by FTIR and ^{1}H NMR giving both similar results. As expected, the FTIR and the ^{1}H NMR spectra for the copolymers are the perfect superposition of the spectra of PMMA and HPDR13. The FTIR spectra of purified DBL and TBL show bands arising from aromatic stretching at 1598 cm^{-1} and NO_2 stretching at 1336 cm^{-1}, from which we can infer the presence of the azomonomer in the chain. The ^{1}H NMR spectrum of the diblock-copolymer DBL-1 is shown in Fig. 3 with the peaks associated with the hydrogen atoms in the sketched molecule.

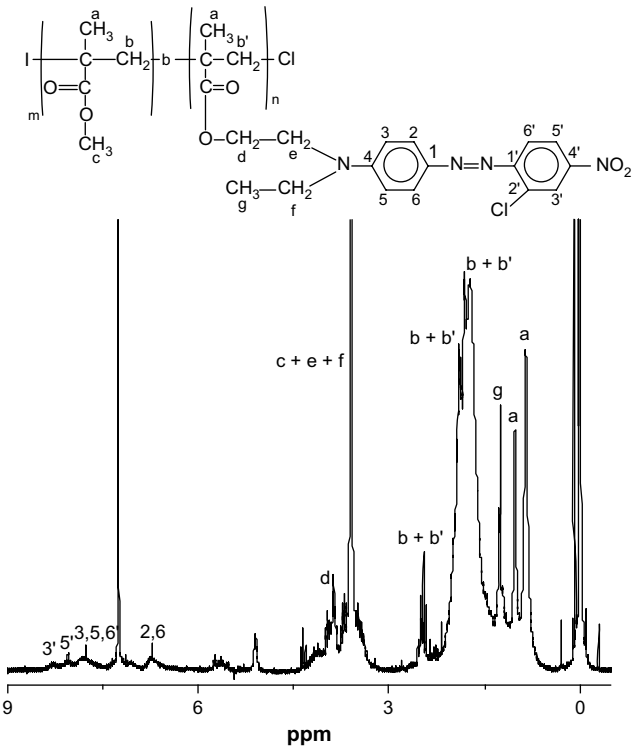

Fig. 3. ^{1}H NMR spectrum of the diblock-copolymer PMMA-*b*-DR13 (DBL) in $CDCl_3$ solvent.

Nuclear magnetic resonance is commonly used to estimate the mass content of each block in copolymers. In our study, however, an accurate analysis is difficult because of the small area of the aromatic peaks (which possesses slow relaxation time) and the overlap of peaks in the 0.5–4.5 ppm region. We therefore estimated the relative concentration of the azo-block with higher accuracy using UV–vis spectroscopy, by comparing the relative absorption at 475 nm of a block-copolymer solution (with known concentration) with a calibration curve built from solutions of the azomonomer in the same solvent. The estimated weight percentage of azo repeating unit was 6.5% for the diblock-copolymer and 12% for the triblock-copolymer.

3.2. Langmuir and LB studies

3.2.1. Homopolymer HPDR13

Langmuir films of HPDR13 were stable at the air/water interface, displaying a surface pressure (π–A) isotherm with two phases (Fig. 4 – circles). At larger areas per repeat unit (33–40 Å^2) one identifies a liquid-expanded phase that is followed by a liquid-condensed phase. The curve is similar to that obtained for HPDR13-conv [30], but the collapse pressure is larger by ca. 10 mN/m. This is likely caused by the linear nature of the ATRP polymer together with its relatively narrow molecular weight distribution, which allows Langmuir films to be stable up to higher surface pressures. UV–vis absorption measurements were taken for HPDR13 Langmuir films *in situ* using the apparatus described in Ref. [35] to investigate aggregation of molecules during compression. The absorption spectrum displayed a maximum at 475 nm, coinciding with that of HPDR13 in solution, in contrast to the case of HPDR13-conv for which the Langmuir film exhibited a red shift in the spectrum due to aggregation. The lack of detectable aggregation in the Langmuir film of HPDR13 is again indicative of polymer chains being amenable to form compact, organized structures. The isotherm for the UV–vis absorption is shown in Fig. 4 (squares), with the signal measured at

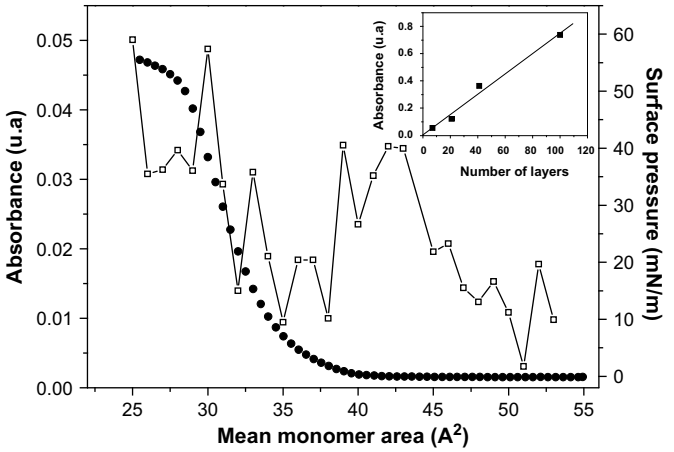

Fig. 4. π–A (circles) and UV–vis (squares) isotherms of HPDR13 obtained by spreading 600 μL of a 0.65 mg/mL chloroform solution. Inset: Plot of the absorbance at 490 nm *versus* number of layers in the LB film.

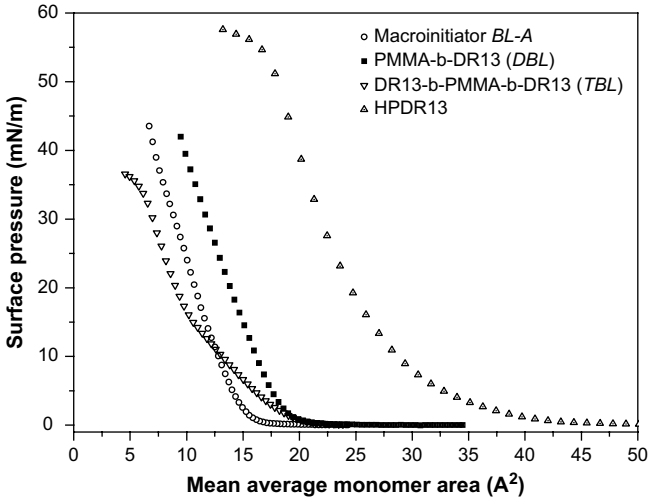

Fig. 5. π–A isotherms of macroinitiator BL-A, diblock-copolymer PMMA-*b*-DR13 (DBL), triblock-copolymer DR13-*b*-PMMA-*b*-DR13 (TBL) and homopolymer HPDR13. Spread volume and solution concentration were as follows: BL-A – 150 μL and 0.54 mg/mL; DBL – 140 μL and 0.40 mg/mL; TBL – 150 μL and 0.50 mg/mL; HPDR13 – 600 μL and 0.65 mg/mL.

475 nm rising at an area where the surface pressure was still zero. This indicates that domain formation begins earlier than it is detected by the surface pressure sensor, a common feature in Langmuir films. This also occurred for HPDR13-conv and reflects structuring of the monolayer leading to drastic changes in the effective dielectric constant at the air/water interface [35]. Absorption of light increased with the film compression as expected by the increase in chromophore density in the light pathway, but the maximum remained at 475 nm, thus indicating negligible chromophores aggregation upon compression.

Homogeneous Langmuir–Blodgett (LB) films up to one hundred layers were transferred from Langmuir films of HPDR13 onto hydrophilic BK7 glass plates. The films were deposited at a constant pressure of 31 mN/m with a typical downward and upward speed of 1 mm/min. The transfer mode was found to be Y-type with a transfer ratio close to 1 up to 10 layers, above which deposition was Z-type, with transfer only during withdrawals of the solid substrate, probably owing to an increase in film roughness and decrease in the substrate/film interactions. Upon transfer some aggregation of chromophores took place, thus shifting the UV–vis absorption spectrum to display a maximum at 490 nm, compared to 475 nm in solution and in the Langmuir films (not shown). The absorption intensity increased linearly with the number of layers effectively transferred as illustrated in the inset of Fig. 4, pointing to the same amount of material being deposited in each layer. As will be shown later, pure LB films of HPDR13 were successfully employed in optical measurements for the first time. HPDR13-conv on its own was not amenable to form good-quality LB films; this was only possible with the aid of film-forming materials such as cadmium stearate. The easier deposition of HPDR13 may be related to the linear feature of the chains, typical of ATRP polymers, and also to its relatively narrow molecular weight distribution, 1.65. This led to a suitable, close packing of the chains with negligible aggregation, yielding high collapse pressures that are advantageous for LB film deposition.

3.2.2. *Block-copolymers PMMA*-b-*DR13 (DBL) and DR13*-b-*PMMA*-b-*DR13 (TBL)*

π–A isotherms for HPDR13, DBL, TBL and the macroinitiator PMMA–Cl (BL-A) are shown in Fig. 5. The isotherm for Cl–PMMA–Cl (BL-B) was omitted as it is similar to that of BL-A. The surface pressure for the diblock-copolymer PMMA-*b*-DR13 (DBL) is intermediate between those for pure HPDR13 and PMMA, as one should expect. Due to the low HPDR13 content in DBL (6.5% in weight), the shape of the curve is similar to that for the PMMA macroinitiator, which is typical of rigid films. Moreover, the extrapolated mean molecular area for DBL, 18.0 Å^2, which roughly represents the area occupied by a repeat unit of the copolymer, is close to that observed for BL-A, ca. 14.5 Å^2. The isotherm for the triblock-copolymer DR13-*b*-PMMA-*b*-DR13 (TBL) displays a similar profile to that for the HPDR13 azo homopolymer, probably due to the high percentage of azo incorporation during the syntheses. It features an initial liquid-expanded phase followed by a liquid-condensed phase that is more compressible than for the macroinitiator BL-A. The collapse pressure was ca. 35 mN/m, smaller than for the homopolymer. The extrapolated mean molecular area was ca. 13.4 Å^2, indicating a higher degree of packing for TBL, with a more condensed film being formed than with the diblock-copolymer.

The data from *in situ* UV–vis experiments for block-copolymers are not shown because the dilution with PMMA caused the signal to be indistinguishable from the noise within the system accuracy. In contrast to the homopolymer, LB films could not be produced from pure PMMA-*b*-DR13 and DR13-*b*-PMMA-*b*-DR13 copolymers. It seems that the less hydrophilic PMMA block hinders chain organization and the transfer of the copolymer as a whole onto the hydrophilic glass slides. We then resorted to the mixed film approach, with co-spread monolayers of cadmiun stearate (CdSt) and DBL or TBL being transferred onto solid substrates for the optical measurements. The surface pressure isotherms for the mixed monolayers were similar to that from the pure polymers regarding shape and areas per repeat unit (results not shown), but the collapse pressures were higher and deposition of the mixed monolayers with CdSt was possible, leading to Y-type LB films with high transfer ratios close to 1.

3.3. *Photoinduced birefringence*

Birefringence was induced in LB films of HPDR13 with no need to use film-forming materials, unlike the case for the HPDR13-conv. Fig. 6 shows a typical optically induced birefringence curve for a 100-layer LB film obtained with a writing laser power of 2.9 mW. The writing laser was switched on at point A and switched off at B. The writing process comprises two steps: a fast initial process due to the alignment of azo moieties, and a second, slower process attributed to the reorientation of chain segments along with the azogroups. After the laser was switched off, some loss of

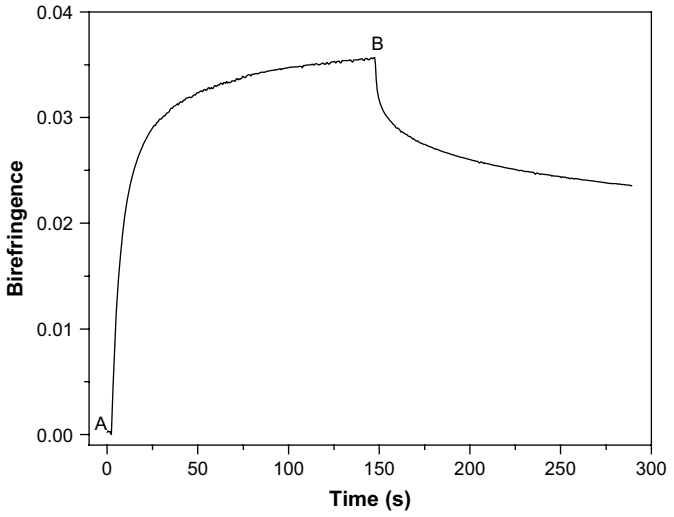

Fig. 6. Optically induced birefringence curve for a 100-layer HPDR13 LB film. The writing laser ($P = 2.9$ mW) was turned on at point A and turned off at point B.

orientation occurred due to thermal effects. The residual birefringence ratio (BR%), defined as the ratio between the residual and maximum birefringence, obtained from Fig. 6 is 66%. The time to achieve 50% of the maximum birefringence ($T_{50\%}$) in Fig. 6 is 7.5 s. It is worth mentioning that the photoinduced birefringence process occurs without sample degradation, as proven in subsidiary experiments where sequential writing–relaxation processes were conducted.

For the pure LB film of HPDR13 the maximum birefringence decreased with increasing number of layers (results not shown). The same trend was observed for azopolymers in mixed LB films co-deposited with cadmium stearate, which was ascribed to the loss of organization in the LB films with a larger number of layers [36]. To further investigate the role played by cadmium stearate in the induced birefringence, we carried out experiments with mixed LB films of the azopolymer HPDR13. For a given measurement under the same conditions as in Fig. 6 (100-layer LB film and $P = 2.9$ mW), $T_{50\%}$ and BR% for the mixed film were 7.0 s and 62%, respectively, which are close to those for the pure LB film in Fig. 6. Nevertheless, the maximum birefringence for the mixed film was 0.009, i.e. one fourth the value for the pure film (ca. 0.035). As the mixed LB film was transferred from 1:1 in weight (CdSt:HPDR13) Langmuir monolayers, one should expect half the value for the birefringence of the pure film. That the maximum birefringence for the mixed film is lower than expected indicates that CdSt has a deleterious effect on the azochromophores. It might be caused by the large size of Cd ions, which may impose constraints to the azochromophore reorientation.

The results from the optically induced birefringence from the LB films of CdSt:HPDR13 can now be compared to those of the mixed LB films made with HPDR13-conv. For the latter, the writing times were shorter and the maximum birefringence considerably higher – almost one order of magnitude – than for the films obtained with HPDR13 synthesized via ATRP. This clearly indicates that the free volume in the highly packed LB films made with HPDR13 is much lower than for the conventionally synthesized HPDR13-conv, which should be expected because there is a trade off between film organization and availability of free volume for the isomerization to occur [4,37]. On one hand, organized LB films tend to give higher birefringence than spin-coated azopolymer films [36,38]. On the other hand, close packing of chromophores prevents them from isomerizing, as was clear in the negligible birefringence measured in LB films of an azobenzene stearate [39]. Indeed, the lack of free

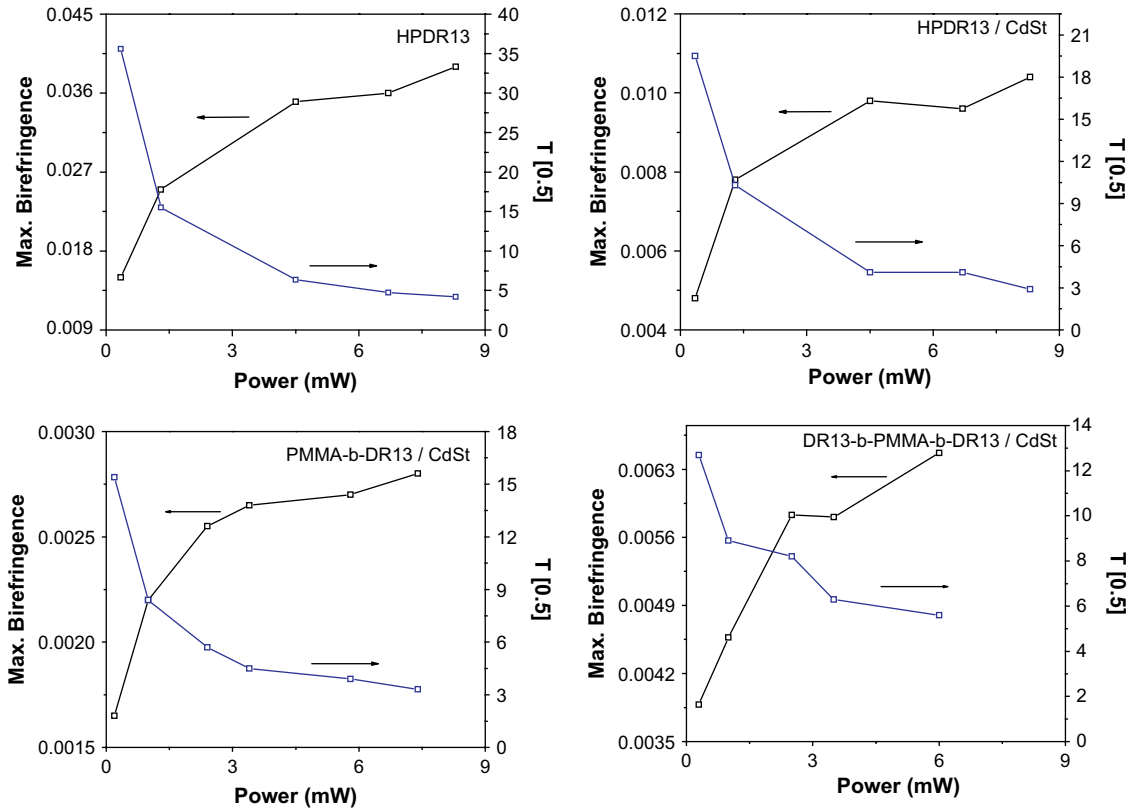

Fig. 7. Maximum birefringence and $T_{50\%}$ *versus* writing laser power for 100-layer Langmuir–Blodgett films of all the materials mixed with cadmium stearate. The maximum birefringence was achieved after 150 s of sample irradiation.

Table 2
$T_{50\%}$ and BR% for the homopolymer HPDR13, diblock-copolymer PMMA-*b*-DR13 (DBL) and triblock-copolymer DR13-*b*-PMMA-*b*-DR13 (TBL), measured for a 100-layer mixed LB film and laser power of 1.0 mW.

Material	$T_{0.5}$ (s)	BR%
HPDR13	10.3	63
DBL	8.4	66
TBL	8.9	56

volume in the CdSt:HPDR13 LB film caused the residual birefringence to be higher than for the CdSt:HPDR13-conv, owing to the difficulty in chromophore relaxation.

The LB films with mixtures of cadmium stearate and block-copolymers investigated here exhibit optical birefringence profiles identical to that of HPDR13. The kinetics of writing consists of a two-step process, analogously to results for HPDR13-conv and PMMA–DR13 random copolymer [40,41], and the results were therefore omitted.

We investigated for all the materials (HPDR13, DBL and TBL) the effect of the writing laser power on the optically induced birefringence. As shown in Fig. 7, the birefringence increased with laser power until saturation was reached at writing laser powers between 7.0 and 9.0 mW. The residual birefringence was almost unaffected, with the values being ca. 62% for the homopolymer HPDR13, ca. 65% for the diblock-copolymer and 57% for the triblock-copolymer. The percentage of residual birefringence is related to structural polymer characteristics as chain mobility or chain entanglement, which remains unaltered. As expected, $T_{50\%}$ values decreased sharply with the writing laser power, as depicted in Fig. 7.

Our main goal was to demonstrate that with the controlled microstructure of block-copolymers one could combine features of DR13-containing polymers and optically inert polymers in a synergistic way. We therefore compared the photoinduced birefringence properties of the homopolymer and the block-copolymers. Since we were not able to produce pure LB films with the diblock- (DBL) and triblock-copolymers (TBL), we used 100-layer LB films of 1:1 (polymer:CdSt) mixtures. The writing laser power was fixed at 1.0 mW. Table 2 shows $T_{50\%}$ and residual birefringence BR% for each compound, from which it is clear that writing times and residual birefringence are similar. The only deviation occurred in the lower value of BR% of TBL, 56%, which may be due to the larger flexibility of the monolayers (see Fig. 5) transferred onto the solid substrates.

In summary, the photoinduced birefringence of the homopolymer in LB films is preserved in the LB films of the copolymers. It is then possible to envisage the combination of these optical properties with the thermal and mechanical characteristics of the PMMA block. Using differential scanning calorimetry we obtained two glass transition temperatures, T_g, of approximately 75 and 115 °C, for the copolymers DBL and TBL. The additional transition at 115 °C represents improved thermal stability for polymer processing in comparison to HPDR13 – obtained either via ATRP or conventional polymerization – whose T_g was ca. 70 °C.

4. Conclusions and prospects for further work

ATRP was used to synthesize the homopolymer HPDR13, leading to samples with lower PDI (1.65) and higher yield (41%) than that obtained in conventional synthesis. This HPDR13 also showed enhanced properties with regard to the film-forming ability, which allowed LB films from the pure polymer to be used for optical storage. From a comparison between LB films of neat HPDR13 and HPDR13 mixed with cadmium stearate, it was possible to infer that cadmium stearate, while assisting in LB film transfer, hampers the chromophore orientation in azopolymers. Also using ATRP, the diblock- (DBL) and triblock-copolymers (TBL) of the azomonomer DR13MA and MMA were synthesized, with enhanced thermal stability in comparison with the azo homopolymer. LB films from mixtures of cadmium stearate and copolymers exhibited basically the same optically induced birefringence features as the LB films of HPDR13. This is promising for practical uses of azopolymers – sometimes hampered in polymer processing by their limited mechanical and thermal properties – for one may combine the optical properties of DR13-containing polymers, and mechanical and thermal properties of PMMA in the same structure.

The improved film-forming ability of the HPDR13 synthesized via ATRP has to do with the higher degree of chain ordering in Langmuir and LB films than is possible for HPDR13-conv. This was inferred from results with Langmuir films, including the negligible chromophores aggregation at the air/water interface and the high collapse pressures. The close packing of the molecules, however, limited the free volume available for isomerization in LB films, thus yielding much lower birefringence than for the films made with HPDR13-conv, and this remains a challenge akin to molecular engineering. Control in molecular structure and film architecture must be sought to allow for organized films, but free volume for chromophores isomerization and reorientation needs to be available. A possible strategy could be the use of copolymers with lower azobenzene concentration, with chromophores attached to a soft block sandwiched between two optically inert blocks.

Acknowledgments

This work was supported by FAPESP, CNPq and IMMP/MCT (Brazil). The authors are also grateful to Prof. Alessandro Gandini (Universidade de Aveiro, Portugal) for the helpful discussions.

References

[1] Oliveira Jr ON, Li L, Kumar J, Tripathy SK. Surface-relief gratings on azobenzene-containing films. In: Sekat Z, Knoll W, editors. Photoreactive organic thin films, 1. San Diego: Academic Press; 2002. p. 429–86.
[2] Meng X, Natansohn A, Rochon P. Polymer 1997;38:2677–82.
[3] Ho MS, Natansohn A, Rochon P. Macromolecules 1995;28:6124–7.
[4] Dall'Agnol F, Silva JR, Zilio SC, Oliveira Jr ON, Giacometti JA. Macromolecular Rapid Communications 2002;23:948–51.
[5] Rochon P, Bissonnette D, Natansohn A, Xie S. Applied Optics 1993;32:7277–80.
[6] Hamley IW. Introduction to block copolymers. In: Hamley IW, editor. Developments in block copolymer science and technology, 1. West Sussex: John Wiley & Sons; 2004. p. 1–29.
[7] Mao G, Wang J, Clingman SR, Ober CK, Chen JT, Thomas EL. Macromolecules 1997;30:2556–67.
[8] Zhao Y, Bai S, Dumont D, Galstian TV. Advanced Materials 2002;14:512–4.
[9] Matyjaszewski K, Xia JH. Chemical Reviews 2001;101:2921–90.
[10] Jiang J, Tong X, Zhao Y. Journal of the American Chemical Society 2005; 127:8290–1.
[11] Tong X, Wang G, Soldera A, Zhao Y. Journal of Physical Chemistry B 2005; 109:20281–7.
[12] Wang G, Tong X, Zhao Y. Macromolecules 2004;37:8911–7.
[13] Ravi P, Sin SL, Gan LH, Gan YY, Tam KC, Xia XL, et al. Polymer 2005;46:137–46.
[14] Sin SL, Gan LH, Hu X, Tam KC, Gan YY. Macromolecules 2005;38:3943–8.
[15] Han YK, Dufour B, Wu W, Kowalewski T, Matyjaszewski K. Macromolecules 2004;37:9355–65.
[16] Cui L, Tong X, Yan X, Liu G, Zhao Y. Macromolecules 2004;37:7097–104.
[17] Yu H, Iyoda T, Ikeda T. Journal of the American Chemical Society 2006; 128:11010–1.
[18] Ruzette AV, Leibler L. Nature Materials 2005;4:19–31.
[19] Lazzari M, Lopez-Quintela MA. Advanced Materials 2003;15:1583–94.
[20] Morikawa Y, Nagano S, Watanabe K, Kamata K, Iyoda T, Seki T. Advanced Materials 2006;18:883–6.
[21] Kadota S, Aoki K, Nagano S, Seki T. Journal of the American Chemical Society 2005;127:8266–7.
[22] Angiolini L, Benelli T, Giorgini L, Salatelli E, Bozio R, Dauru A, et al. Macromolecules 2006;39:489–97.
[23] Tian Y, Watanabe K, Kong X, Abe J, Iyoda T. Macromolecules 2002;35:3739–47.
[24] Frenz C, Fuchs A, Schmidt HW, Theissen U, Haarer D. Macromolecular Chemistry and Physics 2004;205:1246–58.
[25] Angiolini L, Benelli T, Giorgini L, Salatelli E. Polymer 2005;46:2424–32.
[26] Cui L, Zhao Y, Yavrian A, Galstian T. Macromolecules 2003;36:8246–52.
[27] Tong X, Cui L, Zhao Y. Macromolecules 2004;37:3101–12.

[28] Forcén P, Oriol L, Sánchez C, Alcalá R, Hvilsted S, Jankova K, et al. Journal of Polymer Science Part A: Polymer Chemistry 2007;45:1899–910.
[29] Forcén P, Oriol L, Sánchez C, Rodríguez FJ, Alcalá R, Hvilsted S, et al. European Polymer Journal 2007;43:3292–300.
[30] Dhanabalan A, Balogh DT, Riul A, Giacometti JA, Oliveira Jr ON. Thin Solid Films 1998;323:257–64.
[31] Zucolotto V, Strack PJ, Santos FR, Balogh DT, Constantino CJL, Mendonca CR, et al. Thin Solid Films 2004;453–454:110–3.
[32] Matyjaszewski K, Shipp DA, Wang JL, Grimaud T, Patten TE. Macromolecules 1998;31:6836–40.
[33] Teodorescu M, Matyjaszewski K. Macromolecules 1999;32:4826–31.
[34] Rademacher JT, Baum M, Pallack ME, Brittain WJ, Simonsick WJ. Macromolecules 2000;33:284–8.
[35] Dos Santos Jr DS, Pavinatto FJ, Balogh DT, Misoguti L, Oliveira Jr ON, Mendonca CR. Journal of Colloid and Interface Science 2004;276:138–42.
[36] Oliveira Jr ON, Dos Santos Jr DS, Balogh DT, Zucolotto V, Mendonca CR. Advances in Colloid and Interface Science 2005;116:179–92.
[37] Dall'Agnol FF, Oliveira Jr ON, Giacometti JA. Macromolecules 2006;39:4914–9.
[38] Dhanabalan A, Mendonça CR, Balogh DT, Misoguti L, Constantino CJL, Giacometti JA, et al. Macromolecules 1999;32:5277–84.
[39] Dos Santos Jr DS, Mendonça CR, Balogh DT, Dhanabalan A, Cavalli A, Misoguti L, et al. Chemical Physics Letters 2000;317:1–5.
[40] Mendonca CR, Dhanabalan A, Balogh DT, Misoguti L, Dos Santos Jr DS, Pereira da Silva MA, et al. Macromolecules 1999;32:1493–9.
[41] Silva JR, Dall'Agnol FF, Oliveira Jr ON, Giacometti JA. Polymer 2002;43:3753–7.